Mesoporous silica materials labeled for optical oxygen sensing and their application to development of a silica-supported oxidoreductase biocatalyst

Juan M. Bolivar¶, *Sabine Schelch*¶, *Torsten Mayr*⊥, *Bernd Nidetzky*¶‡*

¶ Institute of Biotechnology and Biochemical Engineering, Graz University of Technology, NAWI Graz, Petersgasse 12, A-8010 Graz, Austria

⊥ Institute of Analytical Chemistry and Food Chemistry, Graz University of Technology, NAWI Graz, Stremayrgasse 9, A-8010 Graz, Austria

‡ Austrian Centre of Industrial Biotechnology (acib), Petersgasse 14, A-8010 Graz, Austria

* Corresponding author. Phone: +43 316 873 8400; Fax +43 316 873 8434; E-mail: bernd.nidetzky@tugraz.at

ABSTRACT

Porous silica materials make great supports for heterogeneous catalysis with immobilized enzymes. However, direct functionalization of their surface through stable attachment of enzymes, reporter molecules or both is a difficult problem which to overcome is necessary for practical implementation. Here we integrate the development of luminophor-doped oxygen-sensing silica

materials with a modular strategy of enzyme immobilization to demonstrate generally applicable design of an oxygen-dependent biocatalyst on porous silica support. Z_{basic2}, a highly positively charged silica-binding module of about 7 kDa size, was fused to D-amino acid oxidase and the resulting chimeric protein was tethered noncovalently via Z_{basic2} in defined orientation and in a highly selective manner on silica. The enzyme supports used differed in overall shape and size as well as in internal pore structure. A confocal laser scanning microscopy (CLSM) analysis that employed the oxidase's flavin cofactor as fluorescent reporter group showed homogeneous internal protein distribution in all supports used. Ru-based organometallic luminophor was adsorbed tightly onto the silica supports, thus enabling internal optical sensing of the O_2 available to the enzymatic reaction. Optimization of the surface labeling regarding homogeneous luminophor distribution was guided and its efficacy verified by CLSM. Mesostructured silica surpassed controlled pore glass by ≥ 10-fold in terms of immobilized enzyme effectiveness at high loading of oxidase activity. The effect was shown from detailed comparison of time-resolved O_2 concentration profiles in solution and inside porous support to result exclusively from variable degree of diffusion-caused limitation in internal O_2 availability. Enzyme immobilized on mesostructured silica approached perfection of a heterogeneous biocatalyst in being almost as effective as the free enzyme (assayed in oxidative deamination of D-methionine), thus emphasizing the large benefit of targeted mass transfer intensification, through proper choice of support parameters, in the development of immobilizates of O_2-dependent oxidoreductases on porous silica material.

Keywords: Biocatalysis; oxygen-dependent oxidations; silica materials; enzyme immobilization; fusion protein; silica binding module; optical sensing; intraparticle oxygen gradient

INTRODUCTION

In the chemical sciences the use of enzymes as synthetic catalysts is gaining in importance rapidly[1,2]. Like in chemo-catalysis, enzyme-derived biocatalysts are categorized broadly according to their solubility in the reaction bulk into a homogeneous or heterogeneous class[3–6]. Generally but especially when the scales get bigger, heterogeneous biocatalysts are preferred by virtue of their simplified recycling and all the advantages thus involved [4,5,7]. However, enzymes are normally well soluble in the water-based solvents they require for activity, stability or both. Therefore, making enzymes insoluble constitutes a core task in the development of almost any heterogeneous biocatalyst, the process of which is generally referred to as immobilization[5,7,8]. There exist different principles of enzyme immobilization, but fixation on a solid support is the one most commonly used across scales[5,8,9]. Quest for a suitable support therefore presents critical point of departure in virtually any enzyme immobilization, where the decision made gives direction to the development chain as a whole[6,9]. Besides creating strong opportunities for operating biocatalytic transformations continuously, immobilization on solid support often resulted in enhanced enzyme resistance to various forms of denaturation. This in turn also supports the transition from batch to continuous bioprocessing [10–12].

Considering the chemical-morphological-mechanical-financial tetrad of criteria typically underlying the selection of immobilization supports, silica is expected to emerge as a top candidate, for it is highly biocompatible, readily adjustable in size, stable chemically and incompressible, and also relatively inexpensive[6,13–15]. However, it is noted that silica is not elastic and like many other supports used for enzyme immobilization, it can therefore undergo some abrasion when stirred in suspension. Reason that silica is not widely used for enzyme immobilization at present is difficulty in getting enzymes fixed on the silica surface in a *straightforward* and *practical* manner[6,12–14,16], whereby chemical derivatization of the surface

should be avoided. Availability of supports of a suitable internal pore structure used to be another limitation that has been largely overcome however through the recent advent of mesoporous silica materials[12,17–20]. Identification of protein-based silica binding modules (SBM)[21–25] and demonstration that fusion to SBM constituted a general strategy of designing enzyme chimeras with high affinity for becoming attached to silica surfaces, presented significant progress in the task of making underivatized silica materials readily exploitable for enzyme immobilization[22]. We have shown in recent work that Zbasic2, a strongly positively charged three-helix bundle of about 7 kDa size, presented a highly efficient SBM for the immobilization of different enzymes, including the oxidase used herein and described later[22,23]. Protein attachment to the silica surface of controlled pore glass (CPG) occurred directed via the Zbasic2 module [21,22]. It was also highly selective under stringent immobilization conditions used. Therefore, on offering crude bacterial cell extract for immobilization, it was essentially the target protein containing Zbasic2 that remained bound to the support. By virtue of its noncovalent nature the Zbasic2-silica surface interaction could be tuned through variation in pH and salt concentration to switch from being quasi irreversible during the enzymatic reaction to being readily reversible during regeneration of the support[22]. Finally, multivalency of protein-surface interactions in homooligomeric Zbasic2_enzyme appeared to be useful not only for high-affinity binding but also for oligomer stabilization of the enzyme immobilized[21]. Based on these advances the current study was undertaken to show systematic and comprehensive development of a highly effective O_2-dependent heterogeneous biocatalyst on silica support. Controllable and selective use of O_2 as oxidant in synthetic transformations constitutes an important long-term objective within the chemical sciences[26–35]. A general strategy of creating immobilized enzyme catalysts for that purpose would therefore be highly relevant in the field[36–39].

Development of an immobilized enzyme as heterogeneous biocatalyst would strongly benefit from availability of a suitable process analytical technology[7,13,40]. Therefore, besides directed immobilization on silica via SBM, the current study integrated a second line of recent research from this laboratory on immobilized enzymes, which is the application of optochemical sensing methods for the direct determination of the heterogeneous O_2 environment inside solid supports[41–43]. We have shown in earlier papers how significantly limited the activity of an immobilized oxidase can become as result of reaction-caused depletion of the O_2 substrate within the solid support[42,43]. We have also shown that the degree of internal limitation in O_2 availability constitutes a parameter long sought-after in the rational design of immobilization supports for mass transfer-intensified conversions by O_2-dependent immobilized enzymes[42,43]. However, the supports used in our previous research were all of organic polymer materials such as polymethacrylate. Therefore, a major aim of this study was the development of internally phosphorescently labeled silica materials suitable for O_2 sensing and application of these materials to time-resolved determination of the support-internal O_2 concentration during heterogeneous enzymatic reactions. Thus, different silica materials differing in particle diameter and pore size could be evaluated directly regarding effect of the support parameters on the degree of diffusional limitation. Using D-amino acid oxidase (from the yeast *Trigonopsis variabilis*; DAAO) as a representative and also well-known model enzyme[21,37,44], three silica supports, CPG and the meso-cellular silica foams MSU-VLP and MSU-F[14,45], were examined and selection of the most effective one was demonstrated based on direct evaluation of internal effects of slow O_2 diffusion. Briefly, DAAO is a FAD-dependent enzyme that catalyzes oxidative deamination of an α-D-amino acid substrate coupled to reduction of O_2 into H_2O_2.[44,46] Acting on α-amino acids, DAAO has absolute (D compared to L) enantioselectivity and shows very broad side chain specificity, a combination of

enzyme properties much desired for chiral synthesis of fine chemicals[46,47]. DAAO immobilized via on mesostructured silica presented a unique case where a heterogeneous O_2-dependent biocatalyst approached perfection in being virtually as effective as the free enzyme.

RESULTS AND DISCUSSION

Immobilization of DAAO on Mesoporous Silica Supports

Relevant properties of the silica supports used (CPG, MSU-VLP and MSU-F) are summarized in Table S1 and S2. Besides differences in specific surface area and pore volume, the supports represented significant variation in particle size and pore diameter. Figure 1 and Figure S1 show the differences in particle size. For the purpose of this study, particle size and pore diameter were the key parameters, thus explaining selection of the three supports. Additionally, CPG is very well defined "standard" silica support and direct immobilization of Zbasic2 fusion proteins on it has been studied before. MSU-VLP and MSU-F are highly representative for an emerging class of mesoporous silica materials[14,17]. Note that geometrical properties of the supports are unaltered on changing from dry to wet conditions. The supports do not measurably swell in water.

The previously described DAAO chimera was used that contains Zbasic2 N-terminally fused to the enzyme. Figure 2 shows results of immobilization of Zbasic2_DAAO on the three silica supports. The immobilization was performed stepwise where a protein concentration of 5 g/L was used in solution and an enzyme activity of 400 U (= µmol/min)/g_support was offered in each step. All at once loading was not used to avoid protein aggregation in solution and on the solid surface at high soluble protein concentration. In terms of the immobilization yield, that is, the part

of the offered enzyme activity that was bound, and also the amount of protein loadable, MSU-F was superior to CPG and MSU-VLP, both of which had loading limits at about 2500 U/g_support and 35 mg protein/g_support. With MSU-F, the immobilization yield was complete up to the maximum amount of activity loaded and protein continued to be bound linearly proportional to the amount offered. Note that due to the high selectivity of the immobilization, which is confirmed by analysis with SDS-PAGE of the protein detached from the supports under stringent elution conditions (data not shown), measurement of the bound protein actually represents the amount of Zbasic2_DAAO immobilized. Comparing the binding properties of three supports it is worth noting that the amounts of activity and protein loadable were correlated with the declared specific surface areas of the support, which increases in the order CPG < MSU-VLP < MSU-F. However, there was no correlation between activity and protein loaded and the support's pore size. It is also interesting in view of the approximate molecular dimensions of the homodimeric DAAO (10 nm × 7 nm × 4.5 nm) that the average pore size of 17 nm in MSU-F was still sufficient to allow for enzyme immobilization in high yield (Figure 2).

To characterize the spatial distribution of Zbasic2_DAAO immobilized on the different supports, confocal laser scanning microscopy (CLSM) was used. The fluorescence of the protein-bound FAD cofactor can be detected conveniently without requirement of additional labeling of the enzyme[48,49]. Figure 1 shows representative images collected from each support loaded at approximately 1000 U/g_support. The microscopic evidence reveals that all parts of the solid supports were accessible to Zbasic2_DAAO. Remarkably, this is true even for MSU-F with its relatively narrow pores. Figure 1 and the accompanying Figure S2 in Supporting Information also confirm a largely homogeneous distribution of the immobilized oxidase throughout the solid particle in each support. In trying to establish performance-to-structure correlations for

immobilized enzymes, it is crucial to detect heterogeneity or prove its absence in the internal enzyme distribution. While often assumed to be homogeneous for the sake of simplicity, experimental evidence shows the contrary in various cases where especially under conditions of fast adsorption the actual enzyme distribution on the solid surface featured heterogeneity (e.g. preferred outer-sphere binding) to a large degree [50]. Figure S3 shows the immobilization time course of Zbasic2_DAAO on the different silica supports. On each support binding of the enzyme required over 2 h to be complete. This relatively slow binding probably explains why immobilized enzyme was homogeneously distributed in the solid supports, even the one having small pores (MSU-F). Additionally, MSU-F displays a significant lower particle size, what turns put in lower diffusional distances during protein immobilization.

The comment about FAD release I would rather include in the experimental information. I see it as a caution rather than a result or conclusion.

Characterization of Silica-supported Immobilized Preparations of Zbasic2_DAAO

It is common for an immobilized enzyme that its actual activity is significantly lower than expected from the amount of activity bound to the insoluble support[8,21,43]. Ratio between actual and bound activity is generally referred to as the effectiveness factor (η) of the immobilizate. Figure 3 shows results on analysis of the different Zbasic2_DAAO immobilizates in terms of η. In panel A is shown the dependence of the *actual* activity on the amount of activity offered. Contrary to the dependence of the *bound* activity on activity offered which was linear for all supports up to a loading about 1300 U/g_support (Figure 2), dependence of the actual activity exhibited pronounced curvature already a comparably low enzyme loadings. Effect of leveling out of the actual activity at high enzyme loadings was strongest for CPG but it was also clearly recognized

for MSU-F. Maximum oxidase activity of CPG and MSU-VLP immobilizates was therefore about 200 U/g_support and 600 U/g_support, respectively. Using MSU-F, maximum activity was not reached in the experiment but trend of approaching a "saturated" value was also noticeable for this support. Panel B of Figure 3 compares the three silica supports according to the dependence of η on the immobilizate's actual activity. Overall trend of a decrease in η on increase in activity was present in all supports but there was pronounced difference in magnitude of the effect. For CPG, the drop in η was the most dramatic, resulting in less than 10% effectiveness ($\eta < 0.1$) at low actual activity of only about 250 U/g_support. The declining tendency of η was attenuated in the cellular foam silicas, more strongly so in MSU-F than MSU-VLP. At high level of activity, however, the η values of the two MSU supports appeared to gradually approach each other so that the two immobilizates became similarly effective. Immediate realization from these results was that MSU-L and with certain qualifications MSU-VLP are suitable choices for immobilization of Zbasic2_DAAO. CPG by contrast is completely unsuitable. However, why it was that enzyme immobilizates exhibited such distinctly different η–activity relationship was not clear from the structural characteristics of the silica supports used (Table S1). The effect therefore necessitated more detailed investigation. Based on evidence from CLSM analysis (Figure 1), varying degree of heterogeneity in enzyme distribution within porous support was ruled out as explanation of differences between enzyme immobilizates. Moreover, judging from the value of η at very low actual activity, which was almost unity for the MSU-F immobilizate and still 0.75 for the CPG immobilizate (Figure 3, panel B), Zbasic2_DAAO had not lost a substantial amount of its intrinsic activity in immediate consequence of the attachment to either one of the three silica supports. Indirectly, as argued elsewhere in greater detail, this result supported the suggestion that Zbasic2_DAAO binds to silica surfaces in a highly directed manner via its SBM. Also as proposed

earlier, this orientated binding mode manages to retain the intrinsic activity of the soluble enzyme in the solid immobilizate almost in full, hence $\eta \approx 1$. Additional ramification is that differences in η–activity relationship for the three immobilizates of Zbasic2_DAAO (Figure 3) do not originate from support-specific differences in the binding mode of the enzyme. Variable degree of diffusion limitation was therefore speculated to have caused the individual characteristics of the solid-supported enzyme preparations.

Luminophor Labeling of Silica Supports for Optical Sensing of O_2 in Heterogeneous Environment

To gain direct evidence on the actual availability of dissolved O_2 in the heterogeneous environment of the solid oxidase preparations, we considered an optical sensing approach previously used with enzymes immobilized on organic polymer support. In this approach, tris(4,7-diphenyl-1,10-phenanthroline) ruthenium dichloride[42,43,51,52], in short $Ru(dpp)_3$, was bound to the insoluble support and quenching of the phosphorescence of the immobilized luminophor by O_2 constituted the principle of O_2 measurement[41–43,52]. Critical requirements for application of the method to silica supports were that labeling of the solid surface with $Ru(dpp)_3$ was homogeneous throughout the porous particle and that the luminophor was not leached in water. Optimization of the labeling conditions was necessary to avoid rapid aggregation of $Ru(dpp)_3$ in surface-near regions of the silica particles (Figure S4). Guided by evidence from CLSM analysis as shown in Figure 4 and the accompanying Figure S5 in Supporting Information, the ethanol co-solvent concentrations (10 – 50%, by volume) used during loading and washing of the support as well as the amount of luminophor loaded (1 – 5 mg/g_support) were adjusted such that a labeling with $Ru(dpp)_3$ on the

internal surface of each of the three supports was achieved that was adequate both in *amount* and *uniformity of label distribution* for the intended sensing application.

When incubated under conditions of the enzymatic reaction (50 mM D-Met; pH 8.0; 30 °C; end-over-end mixing) release of luminophor from the silica supports was not detectable over 24 h. Using high NaCl concentration (2 M) in the presence of Tween 80 (0.5%), however, immobilized $Ru(dpp)_3$ was washed off under regeneration of the free support, as shown by CLSM. We confirmed that labeling of the silica supports with $Ru(dpp)_3$ as optimized did not affect the subsequent immobilization of Zbasic2_DAAO regarding both the bound activity and the value of η. The alternative sequence of immobilization where enzyme is immobilized prior to labeling with $Ru(dpp)_3$ was not considered for reason of enzyme inactivation under the labeling conditions where both ethanol co-solvent and ruthenium luminophor were found to be destabilizing for Zbasic2_DAAO[43].

To evaluate the labeled supports for O_2 sensing, luminescence lifetime measurements according to the phase modulation technique[41–43,52] were performed from stirred suspensions of silica particles containing immobilized Zbasic2_DAAO. Figure S6 provides calibration of the analytical signal from each of the three silica supports, showing good correlation between the measured lifetime and the steady-state O_2 concentration. A dynamic range between the approximate limit of quantification of 5 µM and the air-saturated concentration of 250 µM, which was the maximum O_2 concentration used in further experiments, was established for the analytical method. Figure S4 also shows that the labeled silica supports differed in sensitivity in the order MSU-F > MSU-VLP > CPG. Difference in mass-related surface area of the silica supports (Table S1 and Table S2) probably accounted for the effect. Response time of the solid sensor particles was evaluated in assays where consumption of O_2 due to oxidation of L-lactate by soluble L-lactate oxidase was

measured. The [O_2] time course recorded from solid particles was compared to a reference time course measured directly from the liquid phase using a fiber optic sensor. The loading of L-lactate oxidase in solution was varied to change the enzymatic reaction rate. Figure S7 shows that the two corresponding [O_2] time courses were superimposable for each silica support under all conditions used. Therefore, response time of the solid sensor particles was fast enough to avoid time delay in collecting data from the heterogeneous environment relative to the homogeneous liquid phase. Signal-to-noise ratio constitutes a technical detail of the measurement, which we refer to here only briefly. Using particles loaded with $Ru(dpp)_3$ in a mass ratio of 2.5 mg/g_support and applying these particles in a suspended concentration of 2.5 mg_support/mL, luminescence lifetime measurements were of high quality. Lowering the amount of luminophor loaded or working at decreased particle concentration generally resulted in a decrease in the signal-to-noise ratio. In summary, these results demonstrate how the methodological principle of internal sensing of molecular oxygen in porous materials can be extended from organic polymeric supports, to which it was originally restrictedx, to the highly important class of silica supports. Scope of application of the analytical method in heterogeneous bio-catalysis but also heterogeneous chemical catalysis of O_2-dependent transformations is therefore broadened significantly[27,34]. With mesoporous silica materials, an emerging type of catalytic supports is included.

Measurement of the Internal Availability of O_2 During the Heterogeneous Enzymatic Reaction Reveals Effects of Diffusional Limitation

Whenever substrate diffusion is rate limiting in heterogeneously catalyzed reactions, the steady-state substrate concentration in the liquid bulk phase will be higher than the corresponding substrate concentration at a given spatial point in the solid support. Kinetic consequences of substrate depletion from the heterogeneous environment therefore need to be considered for

optimization of an immobilized enzyme. In the case of Zbasic2_DAAO, the enzymatic reaction is kinetically first order with respect to the O_2 concentration, implying that any change in internal [O_2] will proportionally affect the enzymatic rate ("activity"). Experiments were therefore performed to evaluate [O_2] gradients between the bulk phase and the *space-averaged* solid phase during reactions catalyzed by different Zbasic2_DAAO immobilizates on $Ru(dpp)_3$ labeled silica support. The reader is advised to note the space-averaged nature of luminescence lifetime determinations from the solid particles. The [O_2] measured constitutes an averaged concentration over the characteristic particle dimension (e.g. radius of the spheric CPG). Importantly, therefore, the silica supports used were all highly transparent throughout.

Figure 5 shows comparison of time-resolved [O_2] profiles in the external and internal environment of different immobilized oxidase preparations. Major differences between the three silica supports are revealed as result. Using CPG (panel A), a large [O_2] gradient ($\Delta[O_2]$) was formed between liquid bulk and solid support in dependence of reaction time. Note that decrease in the bulk O_2 concentration occurred because gas-liquid O_2-transfer by surface aeration was not significant under these conditions. The enzymatic reaction rate (r_{obs}) was therefore obtained from the data collected from the bulk phase. The $\Delta[O_2]$ increased in clear dependence on the bound oxidase activity (Figure S8), and it was a maximum shortly after the substrate addition. The course of [O_2] in the solid support involved a fast initial decrease of the O_2 level that was followed by a comparably slower O_2 consumption. The second kinetic phase probably reflected the steady state where the rates of O_2 transport into the support and heterogeneous enzymatic reaction had become equal. The maximum value of $\Delta[O_2]$ was determined from the time-resolved [O_2] profiles of different CPG immobilizates, which due to variation in the amount of enzyme loaded gave r_{obs} values in the range 5 – 250 µmol/(min g_support). Figure 6 shows that $\Delta[O_2]$ increased

dramatically in consequence of increase in r_{obs} (panel A) and that η increased as $\Delta[O_2]$ was lowered (panel B).

Used as immobilization supports, the two cellular foam silicas exhibited a behavior pronouncedly different from that of CPG, as shown in Figure 5. Compared at equivalent loading of enzyme activity, development of $\Delta[O_2]$ relative to CPG was strongly attenuated in MSU-VLP and it was almost completely absent in MSU-F ($\Delta[O_2] \leq 10\%$ air saturation). In other words, Zbasic2_DAAO immobilized on MSU-F, and with some qualifications on MSU-VLP, operated in a nearly "pseudo-homogeneous" environment regarding the availability of molecular oxygen for the enzymatic reaction under the conditions used. Employing MSU-VLP as demonstrated in Figure 6 and the accompanying Figure S9 in the Supporting Information, increase in enzyme loading resulted in a gradual increase in the magnitude of the O_2 gradient formed in the enzymatic reaction. The maximum value of $\Delta[O_2]$ increased in response to increase in r_{obs}. Like seen with CPG, the value of η of the enzyme immobilizate of MSU-VLP increased strongly in consequence of a progressing avoidance of drop in the internal O_2 concentration at low r_{obs} (Figure 6, panel B). Diffusional limitations are therefore revealed clearly for the MSU-VLP immobilizates but they are by far less severe than they are in CPG immobilizates. However, in both MSU-VLP and CPG the observed $\Delta[O_2]$ explained quantitatively the declining tendency of η in response to increased loading of enzyme (Figure 3).

The MSU-F immobilizates presented a special case where, as shown in Figure 6 (panel A) and the accompanying Figure S10 in the Supporting Information, the $\Delta[O_2]$ never reached a significant value irrespective of change in r_{obs} between 5 – 800 μmol/(min g_support). A tiny drop of the O_2 concentration in solid support appeared to have occurred (≤ 10% of the value at air saturation;

Figure 6A) but it was always at the very limit of resolution of the analytical method (Figure S8). Therefore, this result implies that the MSU immobilizate was not affected by O_2 diffusion limitation in the range of enzyme loadings examined. That η still decreased at enzyme loadings of 600 μmol/(min g_support) or higher (Figure 3) clearly indicates that the intrinsic activity of Zbasic2_DAAO was affected by the immobilization under these conditions. Investigation of the cause of the effect was beyond the scope of this study but we note that it may equally involve protein concentration-dependent processes on the solid surface and in solution[53].

Heterogeneously Catalyzed Oxidative Deamination of D-Met by Zbasic2_DAAO on Different Silica Supports

We finally examined the three Zbasic2_DAAO immobilizates, each loaded to an activity of 600 μmol/(min g_support), in repeated batchwise conversions of D-Met that involved complete recycling of the solid catalyst after each round of reaction. Surface aeration in combination with suitable catalyst loading was used to ensure that O_2 saturation in bulk was near saturation throughout. Figure 7 shows time courses of the heterogeneously catalyzed reactions and compares them to reaction catalyzed by soluble enzyme. In each reaction, production of α-keto-acid product was approximately linear with time. The productivity increased in the order CPG < MSU-VLP (2-fold) < MSU-F (1.3-fold), as expected from the immobilizates' effectiveness factors (Figure 3 and 6). Productivity of the MSU-F immobilizate was just around 10% less that of the soluble enzyme, indicating an almost perfectly effective immobilized biocatalyst. All solid catalysts were easily separated from the liquid phase by gravity sedimentation and they could be recycled at least three times without appreciable loss in enzyme activity.

CONCLUSIONS

Method of optical sensing of O_2 in the liquid phase within porous silica materials was developed. Effect of diffusion limitation in silica-supported immobilizates of Zbasic2_DAAO was thus made evident directly from experiment. The consequent ability to dissect the main observable of the immobilization (η) into its principal factors, that is, the biocatalytic reaction and the physical transport of O_2, provides a fundamentally advanced approach to the rational development of silica-supported immobilized O_2-dependent biocatalyst. In particular, selection among different candidate solid supports was made possible specifically targeted to the intensification of O_2 mass transport. Direct evidence on the internal (heterogenous) environment of the immobilized Zbasic2_DAAO was absolutely essential in the process, for simple particle parameters such as average pore size and particle diameter exhibited complex correlation with the behavior of the enzyme immobilizates. Huge differences in the silica supports examined herein emphasized the high importance of evidence-based selection of the support material. Compared to standard CPG, enhanced mass transfer in MSU-F resulted in enlargement of the available process window for immobilized Zbasic2_DAAO minimally by about one order of magnitude. The MSU-F immobilizate approached perfection of a heterogeneous biocatalyst in being almost as effective as free enzyme. Overall, the study uses the example of Zbasic2_DAAO to develop a generally applicable design of an O_2-dependent biocatalyst on underivatized porous silica support. Oriented immobilization via the Zbasic2 silica-binding module is employed to create a solid enzyme preparation that offers high intrinsic activity and can be recycled easily. Internal O_2 sensing enables targeted optimization of the immobilizate particularly regarding the degree of diffusional limitation.

EXPERIMENTAL SECTION

Materials

Chimera of D-amino acid oxidase (from *Trigonopsis variabilis*) containing Zbasic2 fused to the enzyme's N-terminus was used. Construction, isolation and characterization of Zbasic2_DAAO were reported recently[23]. *Aerococcus viridans* L-lactate oxidase was a kind gift from Roche Diagnostics (Penzberg, Germany). D-Met, 4-aminoantipyrine, N,N-dimethylaniline, 2,4-dinitrophenylhydrazine, peroxidase from horseradish and glucose oxidase (Type II-S, 15,000-50,000 units/g solid) from *Aspergillus niger* were from Sigma Aldrich GmbH (Vienna, Austria). Dichloride (4,7-diphenyl-1,10-phenantroline)ruthenium(II), in short $Ru(dpp)_3$, was from ABCR GmbH (Karlsruhe, Germany). Glucose was from Roth (Karlsruhe, Germany). Controlled pore glass (Trisoperl®; CPG) was from Vitra Bio GmbH (Steinach, Germany). Mesostructured (cellular foam) silicas MSU-VLP and MSU-F were from InPore Technologies/ DBA Claytec, Inc. (East Lansing, MI, USA). Unless otherwise mentioned, all chemicals were from Sigma (Vienna, Austria) in analytical grade.

Enzyme Assays

Activity of soluble or immobilized DAAO was determined using a peroxidase-coupled assay[21,23]. Direct measurement of the O_2 consumption rate (r_{O2}) was alternatively used for activity determination[43]. Assays were performed at 30 ºC in 50 mM air-saturated potassium phosphate buffer, pH 8.0, using 10 mM D-Met as the substrate. The r_{O2} was measured with a fiber-optic microoptode (Pyroscience GmbH, Aachen, Germany) connected to a fiber optic oxygen meter (model Firesting, Pyroscience). One unit of enzyme activity is the amount of DAAO that produces 1 µmol H_2O_2/min or consumes 1 µmol O_2/min at the conditions used. The enzyme preparations

used had specific activities between 3 µmol/(min mg_protein) for crude cell extract and 70 µmol/(min mg_protein) for purified enzyme.

Luminophor Labeling of Silica Supports

Silica particles were washed with 50 mM potassium phosphate buffer, pH 7.0. The $Ru(dpp)_3$ stock solution in ethanol (2.5 mg/mL) was diluted twofold with buffer and incubated with silica at the concentrations indicated using an end-over-end rotator (20 rpm) for mixing at room temperature (~25 °C). The particle suspension was diluted stepwise with buffer to 10% ethanol and then incubated for 1.5 h under magnetic stirring just strong enough to keep the particles stirred up. Finally, the supports thoroughly were washed with buffer and stored at 4 ºC until further use.

Immobilization of Zbasic2_DAAO

Potassium phosphate buffer, pH 8.0, containing 1.0 M NaCl and 0.5 % (by volume) Tween 20 was used[22]. Immobilization mix contained 50 mg of well washed silica support in a total liquid volume of 1 mL. Besides buffer, the supernatant contained a varied amount of *E. coli* cell extract containing Zbasic2_DAAO. The used enzyme activity varied between 0.05 and 200 U. The protein concentration was between 0.02 and 60 mg/mL. The pH of 8.0 was controlled after addition of enzyme and set when neccessary. Binding to silica support was determined from decrease in activity and protein in solution (supernatant, wash solutions). Immobilization yield is the ratio of activity or protein bound and initially offered. Immobilization to silica proceeded until no further decrease in supernatant occurred. Solid material was then washed with buffer (0.5 M NaCl but no Tween 80; pH 8.0) for 1 h using gentle mixing in the rotator. Second washing was performed identically using buffer containing Tween 80 (0.5 %, by volume) but no NaCl. Immobilizates were stored in 50 mM potassium phosphate buffer, pH 7.0, at 4ºC. Note that enzyme immobilization on

$Ru(dpp)_3$-labeled silica involved buffer containing reduced amounts of NaCl (0.25 M) and Tween 20 (0.01%). The reason was to avoid leaching of the luminophor.

Determination of Catalytic Effectiveness of Immobilized Preparations of Zbasic2_DAAO

The parameter η describes the ratio between the observable activity of the immobilizate and the activity the immobilizate is expected to have from the amount of activity bound to the support. Both activities are expressed in μmol/(min g_support). The observable activity was determined as O_2 consumption rate during conversion of D-Met, measured with a fiber-optic oxygen microoptode (Pyroscience GmbH, Aachen, Germany). Between 0.5 and 25 mg of enzyme immobilizate were resuspended in 4 mL of air-saturated potassium phosphate buffer (50 mM; pH 8.0). An open glass vial (1.2 cm diameter) was placed in a water bath (30°C) and magnetic stirring (6 × 3 mm; 300 rpm) was used. Reaction was started by adding 200 μL of substrate solution (200 mM D-Met) once the O_2 measurement gave a stable signal. Decrease in O_2 was typically followed for about 5 min. It was confirmed by visual inspection that under the stirring conditions used the silica particles were kept completely in suspension and were not mechanically destroyed during the course of the experiment. In addition, the enzyme immobilizate was retained and could be re-used for another round of activity measurement. Successive activity measurements gave fully consistent results. Figure S12 in Supporting Information shows results of an analysis by CLSM in which particles before and after performing a stirring experiment were analyzed.

Determination of Internal O_2 Concentration in Labeled Silica Supports

Phosphorescent signal of labeled silica particles containing or lacking immobilized Zbasic2_DAAO was detected by phase-shift measurements using a miniaturized lock in amplifier (pH-Mini, Presens GmbH, Regensburg, Germany) equipped with a 2-mm optical fiber interfaced

with the reactor[42,43]. Measurements consisted in the determination of the phase shift of the emitted light signal after excitation of the O_2-sensitive $Ru(dpp)_3$ indicator by a sinusoidally intensity modulated light. The phase shift was caused by dynamic luminescence quenching of the indicator depending on the O_2 concentration. Measurements were carried out at a modulation frequency of 45 kHz. The stirred reactor set-up and the conditions were the same as above, except that particle loading was typically between 0.5 and 5.0 mg/mL. Useful signal-to-noise ratios were thus obtained. It was verified through visual inspection that particles were not mechanically destroyed in time span of the experiment. Reaction was started through substrate addition once the system gave at stable phase shift signal and change of phase shift was monitored over time. The Stern-Volmer model was applied to relate experimental phase shifts (and the corresponding phosphorescence lifetimes) on the O_2 concentration. Calibration of the phase shift response was done for each immobilizate separately, as shown in the Supporting Information. Phase shift measurements at various defined O_2 concentrations (adjusted by bubbling with N_2) were performed. Response time of the labeled silica particles was evaluated in experiments where soluble L-lactate oxidase (0.25 - 25 ng/mL) consumed O_2 in bulk due to L-lactate (50 mM) and the resulting decrease in O_2 was monitored through the particle-based phase shift measurement as well as directly in the bulk using the oxygen microsensor described above.

Confocal Laser Scanning Microscopy of Immobilized Zbasic2_DAAO and Labeled Silica Supports

About 30 µL of luminophor-labeled and enzyme-immobilized silica support (10 mg/mL) suspended in 50 mM potassium phosphate buffer, pH 7.0, were placed in a microscope slide mounted with a cover slip. Confocal images were acquired using a Leica DM5500Q microscope system (Mannheim, Germany) equipped with an objective for 63-fold magnification (ACS APO

63×/1.30 OIL). For imaging of the flavin cofactor of Zbasic2_DAAO, excitation was at 405 nm and emitted light was collected in the range 480 - 650 nm. Notice that the imaging of FAD was performed immediately after the preparation of immobilized Zbasic2_DAAO to discard any effect of FAD release from the immobilized Zbasic2_DAAO; data of activity conservation of free enzyme during timespan of immobilization experiments and values of catalytic effectiveness of immobilized Zbasic2_DAAO supports the idea of a conservation of a protein-bound FAD. $Ru(dpp)_3$ imaging, excitation was at 488 nm and the emitted light was collected in the range 500 - 694nm. Images were processed using Fiji imageJ processing package software. Bright field pictures were acquired using a Leica DFC360FX CCD camera connected to the microscope.

Repeated Batchwise Oxidation of D-Met by Immobilizates of Zbasic2_DAAO Using Recycling of Solid Catalyst

Reactions consisted of 1 mL solution (50 mM D-Met; 50 mM potassium phosphate, pH 8.0) containing 0.33 mg immobilizate/mL (bound activity: 600 U/g_support) or 0.2 U/mL of free enzyme. Catalase from bovine liver (4000 U/mg) was added at 0.1 mg protein/mL to ensure the decomposition of hydrogen peroxide formed[54]. Incubation was done in Eppendorf tubes at room temperature (~25 °C) and an end-over-end-rotator (20 rpm) was used for mixing. O_2 availability in supernatant (~90 % air saturation at atmospheric pressure) was regularly checked using measurement with the oxygen microoptode. At indicated times, a homogeneous sample was withdrawn and the concentration of 2-keto-4-(methylthio)butyric was determined. Reaction progress was followed for 6 h. At the end, the enzyme immobilizate was recovered by sedimentation, and it was used again for two new rounds of conversion. Quantification of 2-keto-4-(methylthio)butyric was performed as described elsewhere[55,56] with some modifications. Briefly,

50 µL of sample and the same volume of 2,4-dinitrophenylhydrazine (DNP) solution (1.0 mM of DNP in 2 M HCl) were mixed and incubated at room temperature for 10 min. Subsequently, 200 µL of 1.5 M NaOH were added, mixed and incubated for an additional 10 min. Finally, 200 µL of the mixture were diluted in the same volume of 50 mM potassium phosphate, pH 7.0, and the absorbance was read at 440 nm. A blank was also measured under the same conditions but using 50 mM D-Met in 50 mM potassium phosphate, pH 8.0 instead of the sample solution.

Data Analysis and Presentation

The data shown are averages of three or more independent experiments. Mean values and their standard deviations are given in text and figures.

FIGURES

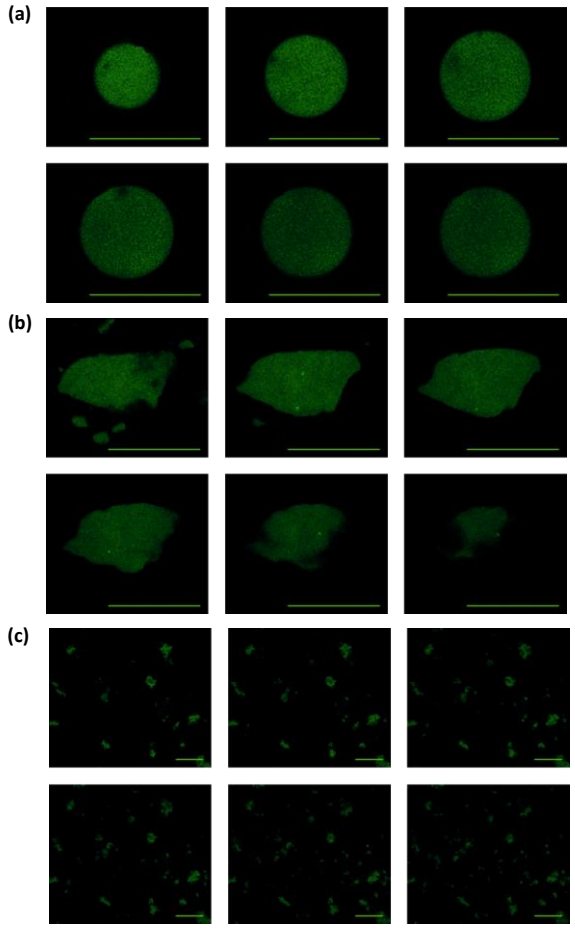

Figure 1. Confocal fluorescence images of Z_{basic2}_DAAO immobilized on silica supports. (a) CPG; (b) MSU-VLP; and (c) MSU-F. The scale bar indicates 100 µm in (a) and (b), and 20 µm in (c). Images were obtained by taking different z-section scans with a 0.33 µm (c) and a 4.99 µm (a, b) depth margin between each image.

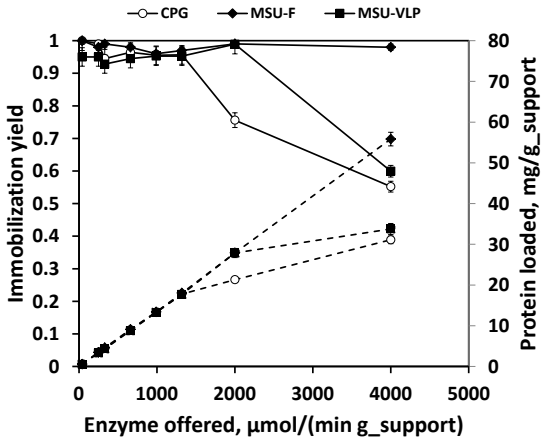

Figure 2. Immobilization of Z_{basic2}_DAAO on silica supports is shown. Immobilization yield is the ratio of bound and initially offered enzyme activity. It is shown in full lines. Dashed lines show the protein loaded on the support. The supports are indicated by symbols. For more details, see the Experimental Section.

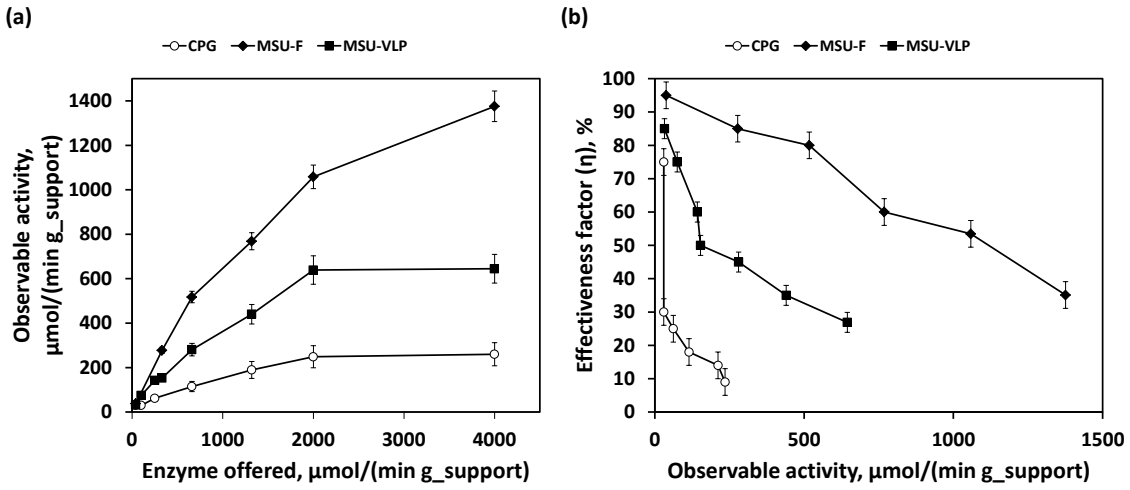

Figure 3. Observable activity (a) and catalytic effectiveness (b) of Zbasic2_DAAO immobilizates in the oxidation of D-Met are shown. The observable activity represents the initial rate of O_2 consumption in bulk solution. The catalytic effectiveness is the ratio between the observable activity and the activity bound to the support. Bound activity is the product of immobilization yield and offered activity. Reactions were performed at 30 ºC using air-saturated potassium phosphate buffer (50 mM; pH 8.0). For more details, see the Experimental Section.

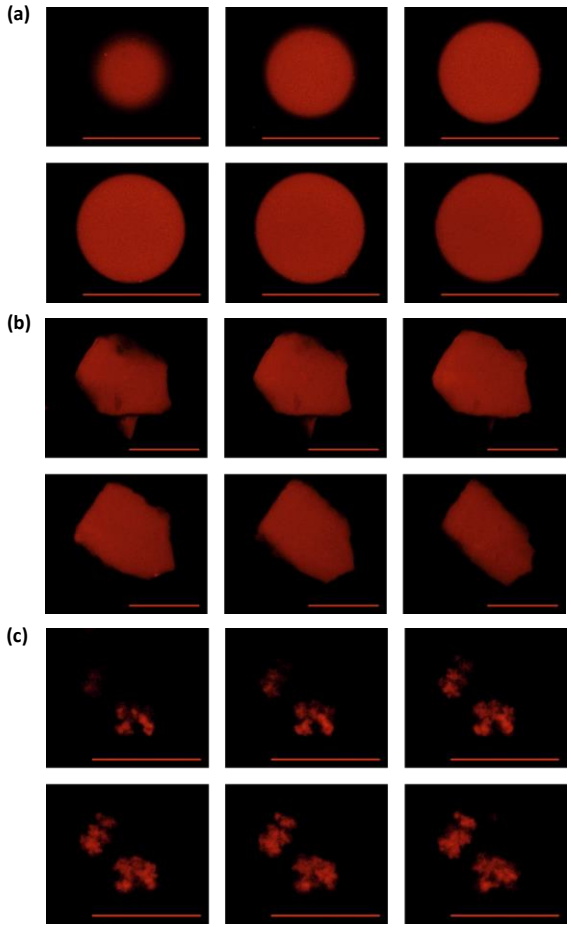

Figure 4. Confocal fluorescence images of silica supports labeled with $Ru(dpp)_3$. (a) CPG; (b) MSU-VLP; (c) MSU-F. The scale bar indicates 100 μm in (a) and (b), and 20 μm in (c). Images were obtained by taking different z-section scans with a 0.33 μm (c) and a 4.99 μm (a, b) depth margin between each image.

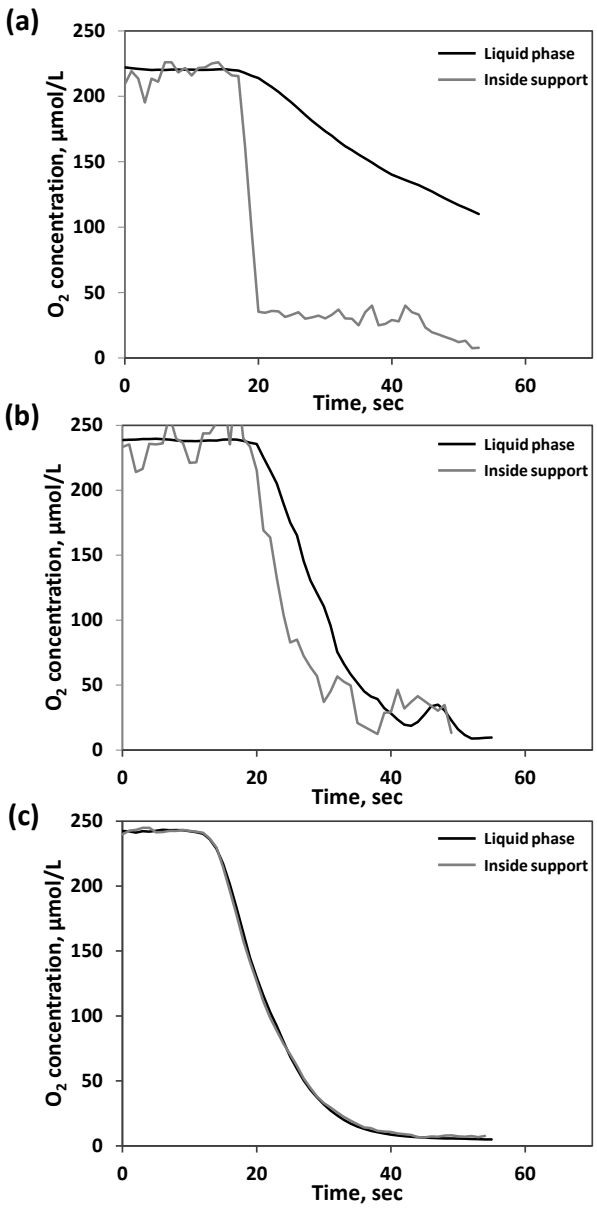

Figure 5. Time courses of the O_2 concentration in liquid phase and inside porous support during oxidation of D-Met by different Z_{basic2}_DAAO immobilizates. Each support was loaded with 600 µmol/(min g_carrier), and 5 mg_carrier/mL were used in the reaction. (a) CPG; (b) MSU-VLP; (c) MSU-F. Reactions were performed at 30 ºC using air-saturated potassium phosphate buffer(50 mM; pH 8.0). For more details, see the Experimental Section.

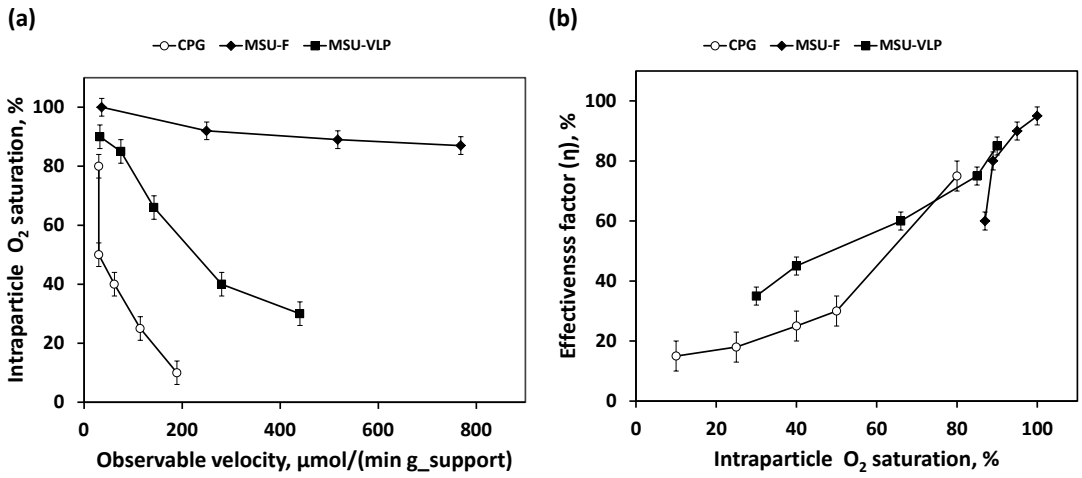

Figure 6. (a) Dependence of the O_2 concentration inside the porous support (at apparent steady state) on the observable velocity of D-Met oxidation by the Zbasic2_DAAO immobilizate, and (b) dependence of the effectiveness factor of the immobilizate on O_2 concentration inside the porous support. Reactions were performed at 30 ºC using air-saturated potassium phosphate buffer (50 mM; pH 8.0). For more details, see the Experimental Section.

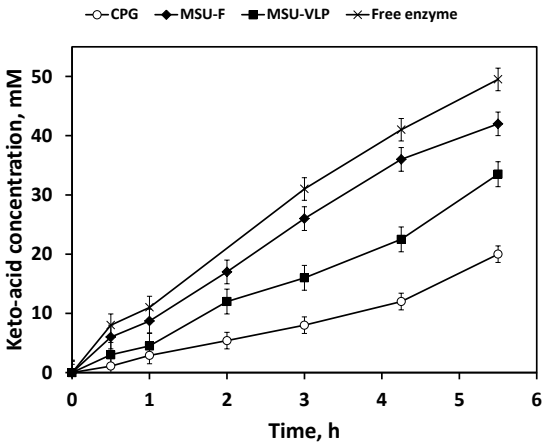

Figure 7. Batchwise oxidation of D-Met (50 mM) into 2-keto-4-(methylthio)butyric acid using soluble or silica-supported preparations of Zbasic2_TvDAO at equivalent volumetric enzyme loading of 0.2 μmol/(min mL). Catalase (400 U/mL) was added to destroy H_2O_2, to partly regenerate O_2 and to prevent α-keto-acid decarboxylation. The symbols indicate soluble enzyme (asterisk) and immobilizates on CPG (open circles), MSU-VLP (squares), and MSU-F (diamonds). Note that immobilizates were recycled for two new rounds of reaction, giving the same performance each time. For more details, see the Experimental Section.

ASSOCIATED CONTENT

Supporting Information. A summary of properties of the silica supports used (Table S1 and S2); supporting SEM images of supporting meso-cellular foams supports used (Figure S1); supporting CLSM images of Zbasic2_DAAO immobilized on the different silica supports (Figure S2); supporting immobilization time course of Zbasic2_DAAO on the different silica supports (Figure S3); supporting CLSM images showing aggregation of ruthenium luminophor in CPG support (Figure S4); supporting CLSM images showing immobilization of ruthenium luminophor ion the different silica supports (Figure S5); Stern-Volmer plot correlating luminescence lifetime recorded from labeled silica supports and the O_2 concentration in bulk liquid (Figure S6); response time analysis of labeled silica supports under conditions of O_2-dependent enzymatic reaction in solution (Figure S7); time-resolved profiles of O_2 concentration in the bulk liquid phase and in solid particle for reactions by Zbasic2_DAAO immobilized on CPG (Figure S8), MSU-VLP (Figure S9) and MSU-F (Figure S10); determination of the maximum value of ΔO_2 in reactions catalyzed by different DAAO immobilizates (Figure S11); supporting CLSM images comparing silica supports before and after use in stirring experiments (Figure S12). This material is available free of charge via the Internet at http://pubs.acs.org.

AUTHOR INFORMATION

Corresponding Author

*Prof. Bernd Nidetzky, Institute of Biotechnology and Biochemical Engineering, Graz University of Technology, NAWI Graz, Petersgasse 12, A-8010 Graz, Austria; phone: +43 316 873 8400; fax: +43 316 873 8434; e-mail: bernd.nidetzky@tugraz.at

Author Contributions

The manuscript was written through contributions of all authors. All authors have given approval to the final version of the manuscript. JMB and BN designed the research. JMB and SS performed experiments and analyzed data. TM contributed to development of analytical procedures. JMB and BN wrote the paper.

ACKNOWLEDGMENT

Dr. Zdenek Petrasek (Institute of Biotechnology and Biochemical Engineering) assisted the CLSM experiments and Prof. Thomas J. Pinnavaia (InPore Technologies/ DBA Claytec, Inc) provided technical data about the silica supports used. Dr. Victoria Gascon (group of Molecular Sieves, Institute of Catalysis and Petrochemistry, CSIC, Madrid) provided the structural characterization of meso-cellular foams supports used.

ABBREVIATIONS

CLSM, confocal laser scanning microscopy; SEM, Scanning electron microscope; CPG, controlled pore glass; DAAO, D-amino acid oxidase; Zbasic2_DAAO, DAAO containing Zbasic2 fused as SBM to the enzyme's N-terminus.

REFERENCES

(1) Torrelo, G.; Hanefeld, U.; Hollmann, F. *Catal. Lett.* **2015**, 145, 309–345.

(2) Clouthier, C. M.; Pelletier, J. N. *Chem. Soc. Rev.* **2012**, 41, 1585–1605.
(3) Guisán, J. M. *Immobilization of enzymes and cells*; Humana Press: Totowa, New Jersey, 2010; pp 1-13.
(4) Buchholz, K.; Kasche, V.; Bornscheuer, U. T. *Biocatalysts and enzyme technology*; Wiley-VCH, Weinheim, 2005; pp 243-282.
(5) Hanefeld, U.; Cao, L.; Magner, E. *Chem. Soc. Rev.* **2013**, 42, 6211–6212.
(6) Tran, D. N.; Balkus, K. J. *ACS Catal.* **2011**, 1, 956–968.
(7) Liese, A.; Hilterhaus, L. *Chem. Soc. Rev.* **2013**, 42, 6236.
(8) Garcia-Galan, C.; Berenguer-Murcia, Á.; Fernandez-Lafuente, R.; Rodrigues, R. C. *Adv. Synth. Catal.* **2011**, 353, 2885–2904.
(9) Cantone, S.; Ferrario, V.; Corici, L.; Ebert, C.; Fattor, D.; Spizzo, P.; Gardossi, L. *Chem. Soc. Rev.* **2013**, 42, 6262–6276.
(10) Sheldon, R. A.; van Pelt, S. *Chem. Soc. Rev.* **2013**, *42* (15), 6223–6235
(11) Rodrigues, R. C.; Ortiz, C.; Berenguer-Murcia, Á.; Torres, R.; Fernández-Lafuente, R. *Chem.* Soc. *Rev.* **2013**, *42* (15), 6290–6307
(12) Magner, E. *Chem. Soc. Rev.* **2013**, 42 , 6213–6222
(13) Carlsson, N.; Gustafsson, H.; Thörn, C.; Olsson, L.; Holmberg, K.; Åkerman, B. *Adv. Colloid Interface Sci.* **2014**, 205, 339–360.
(14) Hartmann, M.; Kostrov, X. *Chem. Soc. Rev.* **2013**, 42, 6277–6289.
(15) Hartmann, M. *Chem. Mater.* **2005**, 17, 4577–4593.
(16) Gaffney, D.; Cooney, J.; Magner, E. *Top. Catal.* **2012**, 55 , 1101–1106.
(17) Zhou, Z.; Hartmann, M. *Chem. Soc. Rev.* **2013**, 42, 3894–3912.
(18) Gascón, V.; Díaz, I.; Márquez-Álvarez, C.; Blanco, R. M. *Mol. Basel Switz.* **2014**, 19, 7057–7071.
(19) Bernal, C.; Sierra, L.; Mesa, M. *ChemCatChem* **2011**, 3, 1948–1954.
(20) Bernal, C.; Illanes, A.; Wilson, L. *Langmuir* **2014**, 30, 3557–3566.
(21) Bolivar, J. M.; Nidetzky, B. *Biotechnol. Bioeng.* **2012**, 109, 1490–1498.
(22) Bolivar, J. M.; Nidetzky, B. *Langmuir* **2012**, 28, 10040–10049.
(23) Wiesbauer, J.; Bolivar, J. M.; Mueller, M.; Schiller, M.; Nidetzky, B. *ChemCatChem* **2011**, 3, 1299–1303.
(24) Ikeda, T.; Kuroda, A. *Colloids Surf. B Biointerfaces* **2011**, 86, 359–363.
(25) Ikeda, T.; Motomura, K.; Agou, Y.; Ishida, T.; Hirota, R.; Kuroda, A. *Protein Expr. Purif.* **2011**, 77, 173–177.
(26) Sheldon, R. A.; Arends, I. W. C. E.; Ten Brink, G.-J.; Dijksman, A. *Acc. Chem. Res.* **2002**, 35, 774–781.
(27) Sheldon, R. A. *Catal. Today* **2015**, 247, 4–13.
(28) Shi, Z.; Zhang, C.; Tang, C.; Jiao, N. *Chem. Soc. Rev.* **2012**, 41, 3381–3430.
(29) Podgoršek, A.; Zupan, M.; Iskra, J. *Angew. Chem. Int. Ed.* **2009**, 48, 8424–8450.
(30) Chen, B.-T.; Bukhryakov, K. V.; Sougrat, R.; Rodionov, V. O. *ACS Catal.* **2015**, 5, 1313–1317.
(31) Schümperli, M. T.; Hammond, C.; Hermans, I. *ACS Catal.* **2012**, 2, 1108–1117.
(32) Que, L.; Tolman, W. B. *Nature* **2008**, 455, 333–340.
(33) Punniyamurthy, T.; Velusamy, S.; Iqbal, J. *Chem. Rev.* **2005**, 105, 2329–2363.
(34) Mallat, T.; Baiker, A. *Chem. Rev.* **2004**, 104, 3037–3058.
(35) Davis, S. E.; Ide, M. S.; Davis, R. J. *Green Chem* **2013**, 15, 17–45.

(36) Hollmann, F.; Arends, I. W. C. E.; Buehler, K.; Schallmey, A.; Bühler, B. *Green Chem* **2011**, 13, 226–265.
(37) Turner, N. J. *Chem. Rev.* **2011**, 111, 4073–4087.
(38) Monti, D.; Ottolina, G.; Carrea, G.; Riva, S. *Chem. Rev.* **2011**, 111, 4111–4140.
(39) Hall, M.; Bommarius, A. S. *Chem. Rev.* **2011**, 111, 4088–4110.
(40) Bolivar, J. M.; Eisl, I.; Nidetzky, B. *Catal. Today* In press 10.1016/j.cattod.2015.05.004.
(41) Bolivar, J. M.; Consolati, T.; Mayr, T.; Nidetzky, B. *Trends Biotechnol.* **2013**, 31, 194–203.
(42) Bolivar, J. M.; Consolati, T.; Mayr, T.; Nidetzky, B. *Biotechnol. Bioeng.* **2013**, 110, 2086–2095.
(43) Bolivar, J. M.; Schelch, S.; Mayr, T.; Nidetzky, B. *ChemCatChem* **2014**, 6, 981–986.
(44) Pollegioni, L.; Molla, G.; Sacchi, S.; Rosini, E.; Verga, R.; Pilone, M. S. *Appl. Microbiol. Biotechnol.* **2008**, 78, 1–16.
(45) Linssen, T.; Cassiers, K.; Cool, P.; Vansant, E. F. *Adv. Colloid Interface Sci.* **2003**, *103* (2), 121–147
(46) Pilone, M. S.; Pollegioni, L. *Biocatal. Biotransformation* **2002**, *20* (3), 145–15(42) (46)
(47) Turner, N. J. *Chem. Rev.* **2011**, *111* (7), 4073–4087
(48) Tanaka, F.; Tamai, N.; Yamazaki, I.; Nakashima, N.; Yoshihara, K. *Biophys. J.* **1989**, *56*, 901-909
(49) van den Berg, P.A.W.; Visser, A. J. W. G. in *New Trends in Fluorescence Spectroscopy Applications to* Chemical *and Life Sciences*; Valeur, B.; Brochon, J.-C., Eds; Springer Berlin Heidelberg: Berlin, Heidelberg, 2001; pp 457-459
(50) Bolivar, J. M.; Hidalgo, A.; Sánchez-Ruiloba, L.; Berenguer, J.; Guisán, J. M.; López-Gallego, F. *J. Biotechnol.* **2011**, 155, 412–420.
(51) Quaranta, M.; Borisov, S. M.; Klimant, I. *Bioanal. Rev.* **2012**, 4, 115–157.
(52) Papkovsky, D. B.; Dmitriev, R. I. *Chem. Soc. Rev.* **2013**, 42, 8700–8732.
(53) Secundo, F. *Chem. Soc. Rev.* **2013**, 42, 6250–6261.
(54) Hernandez, K.; Berenguer-Murcia, A.; C. Rodrigues, R.; Fernandez-Lafuente, R. *Curr. Org. Chem.* **2012**, *16* (22), 2652–2672
(55) Oguri, S.; Watanabe, K.; Nozu, A.; Kamiya, A. *Food Chem.* **2007**, 100, 616–622.
(56) Nuutinen, J. T.; Timonen, S. *Mycol. Res.* **2008**, 112, 1453–1464.

Table of Contents Graphic and Synopsis

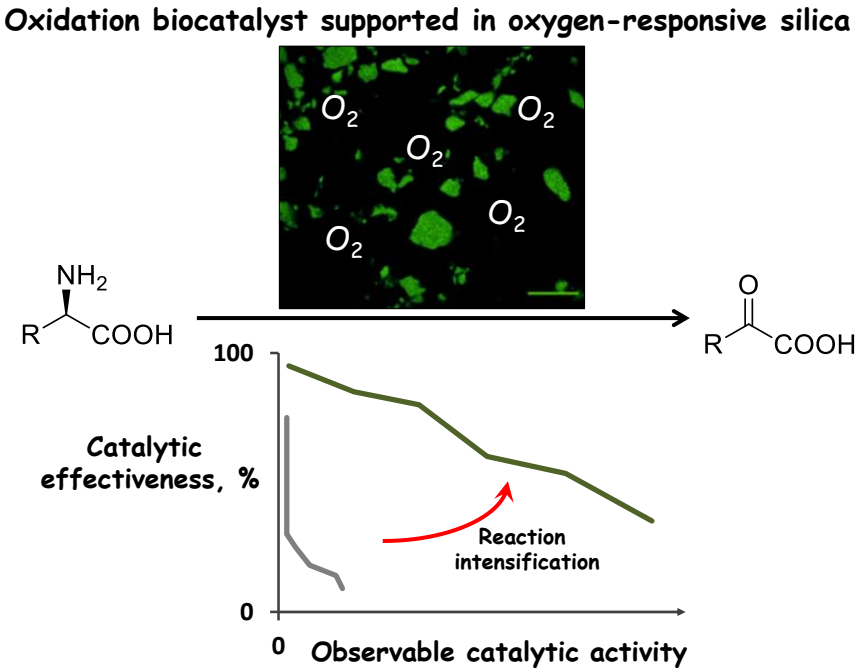

Using luminophor labeling of silica material for optical sensing of O_2, generally applicable approach for development of highly active silica-supported O_2-dependent oxidoreductase (here: D-amino acid oxidase) biocatalysts is reported. Oriented immobilization via a silica binding module ensures retention of high specific activity in the enzyme immobilizate, and direct evidence on the O_2 available in the heterogeneous environment supports targeted selection of an insoluble support with intensified O_2 mass transfer characteristics.

Supporting information

Mesoporous silica materials labeled for optical oxygen sensing and their application to development of a silica-supported oxidoreductase biocatalyst

Juan M. Bolivar¶, *Sabine Schelch*¶, *Torsten Mayr*⊥, *Bernd Nidetzky*¶‡*

¶ Institute of Biotechnology and Biochemical Engineering, Graz University of Technology, NAWI Graz, Petersgasse 12, A-8010 Graz, Austria

⊥ Institute of Analytical Chemistry and Food Chemistry, Graz University of Technology, NAWI Graz, Stremayrgasse 9, A-8010 Graz, Austria

‡ Austrian Centre of Industrial Biotechnology (acib), Petersgasse 14, A-8010 Graz, Austria

* Corresponding author. Phone: +43 316 873 8400; Fax +43 316 873 8434; E-mail: bernd.nidetzky@tugraz.at

SUPPORTING TABLES

Table S1. Technical specifications of silica supports. Data were kindly provided by VitraBio GmbH for CPG and InPore Technologies/DBA Claytec, Inc. for cellular foam materials.

Support	Particle size, µm	Pore size, nm	Pore volume, mm^3/g	Specific area, m^2/g
CPG (Trisoperl®)	50-100	161	1521	43
Mesostructured (cellular foam) silica MSU-VLP	5-140	67	1200	172
Mesostructured (cellular foam) silica MSU-F	3-7	17	1700	481

Table S2. Textural and structural parameters of the cellular foam silica supports used.

Support	Pore size, nm [a]	Entrance size, nm [b]	Pore volume, mm^3/g [c]	Specific area, m^2/g [d]
Mesostructured (cellular foam) silica MSU-VLP	10-80 [a1]	10-40	800	161
Mesostructured (cellular foam) silica MSU-F	15	12	1500	445

[a] The pore size was calculated from the *adsorption branch* of the N_2 adsorption/desorption isotherms based on the Barrett-Joyner-Halenda (BJH) model. [a1] The pore distribution was very wide.

[b] The entrance size was calculated from the *desorption branch* of the N_2 adsorption/desorption isotherms based on BJH model.

[c] The pore volume was estimated from the amount of nitrogen adsorbed at the relative pressure of (p/p_0) of 0.98 (p_0 is the saturation pressure of nitrogen at the adsorption temperature).

[d] Specific surface area (m^2/g) determined from the linear part of the Brunauer-Emmett-Teller equation.

Nitrogen adsorption-desorption isotherms of the samples were measured at -196 ºC using a Micromeritics ASAP 2420 volumetric adsorption analyser. Samples were outgassed at 350 ºC for 16 h under high vacuum before measurement.

SUPPORTING FIGURES

(a)

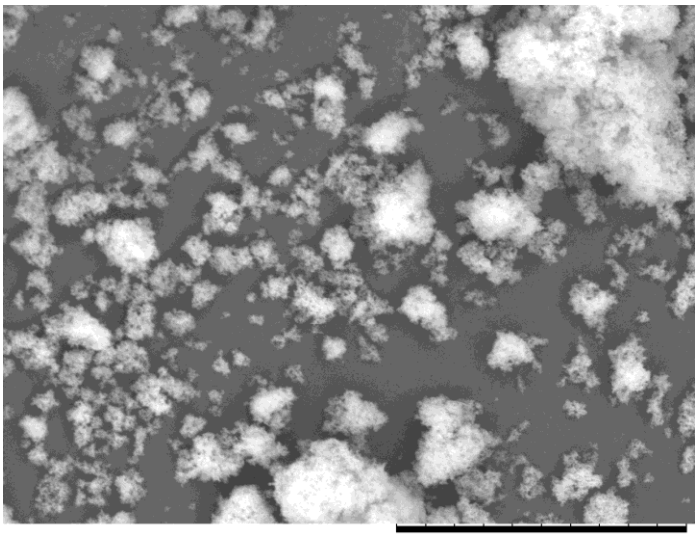

(b)

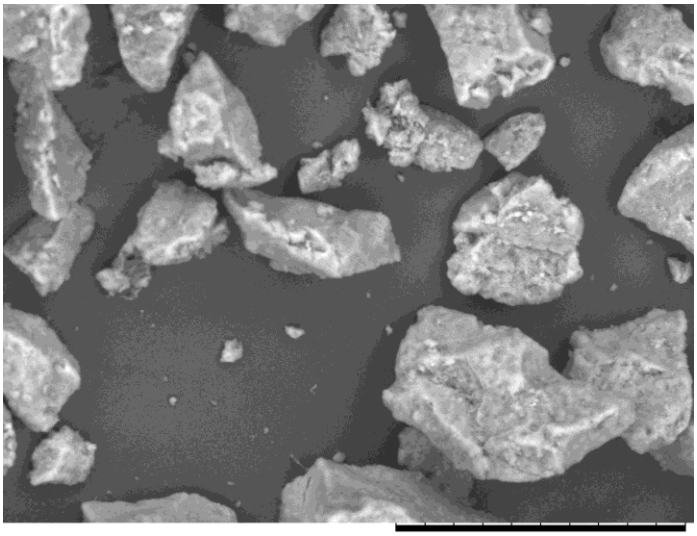

Figure S1. SEM micrographs of cellular foam silica supports. (a) MSU-F; (b) MSU-VLP. The scale bar on the picture indicates a width of 200 MSU-VLP and a width of 100 μm for MSU-F.The particle morphologies of the prepared mesoporous silica were examined by scanning electron microscopy (SEM). Images were collected using a FE-SEM FEI Nova Nanosem 230 microscope with vCD detector. The samples for SEM analysis were prepared by placing material powder on double-sided graphite adhesive tape mounted on the sample holder.

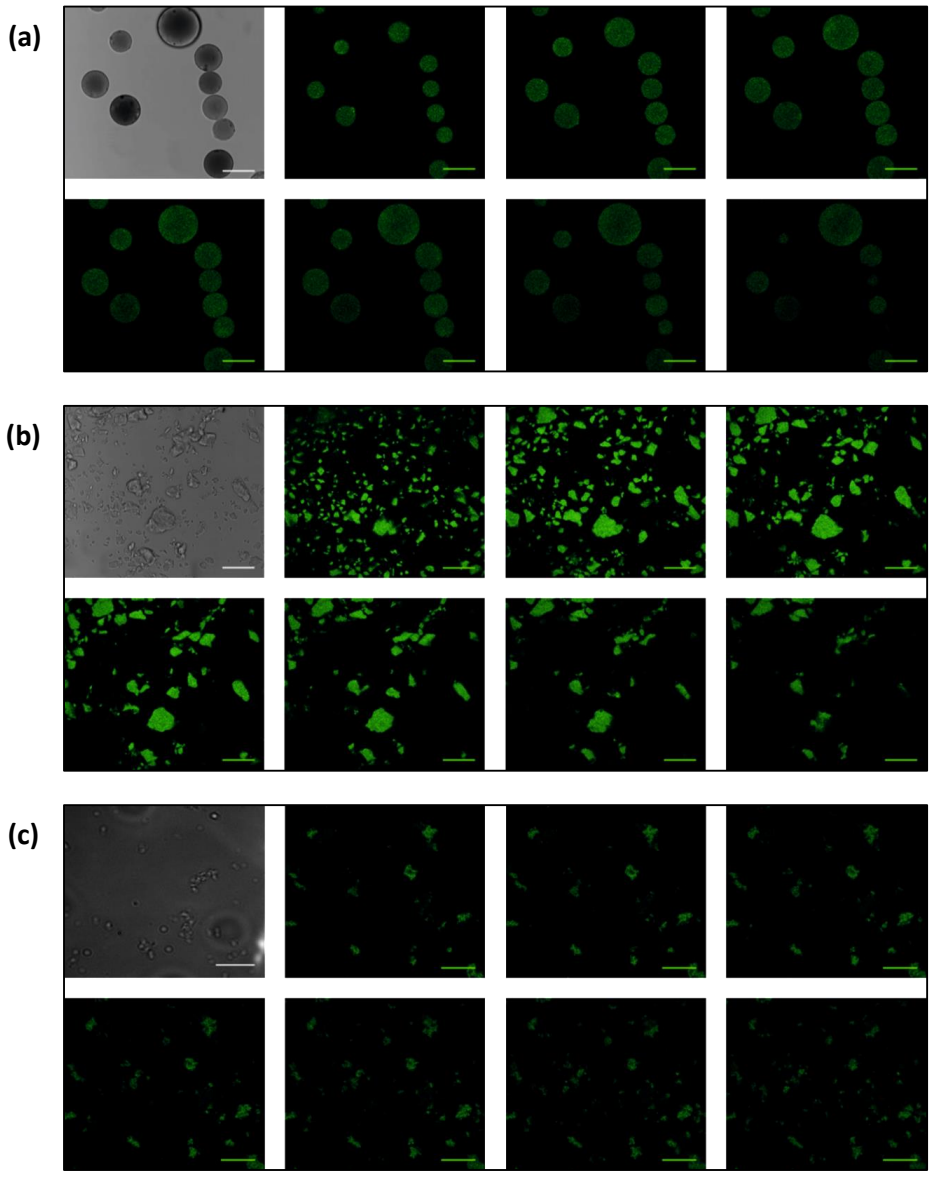

Figure S2. Images of Z_{basic2}_DAAO immobilized on silica supports. (a) CPG; (b) MSU-VLP; (c) MSU-F. The scale bar on the picture indicates a width of 100 µm for CPG and MSU-VLP and a width of 20 µm for MSU-F. The first picture of each panel shows a transmission microscope image. The following pictures of each panel show fluorescence confocal images. The confocal fluorescence images were obtained by taking different z-section scans with 0.33 (for MSU-F) or 4.99 µm (for CPG and MSU-VLP) depth margin between each image.

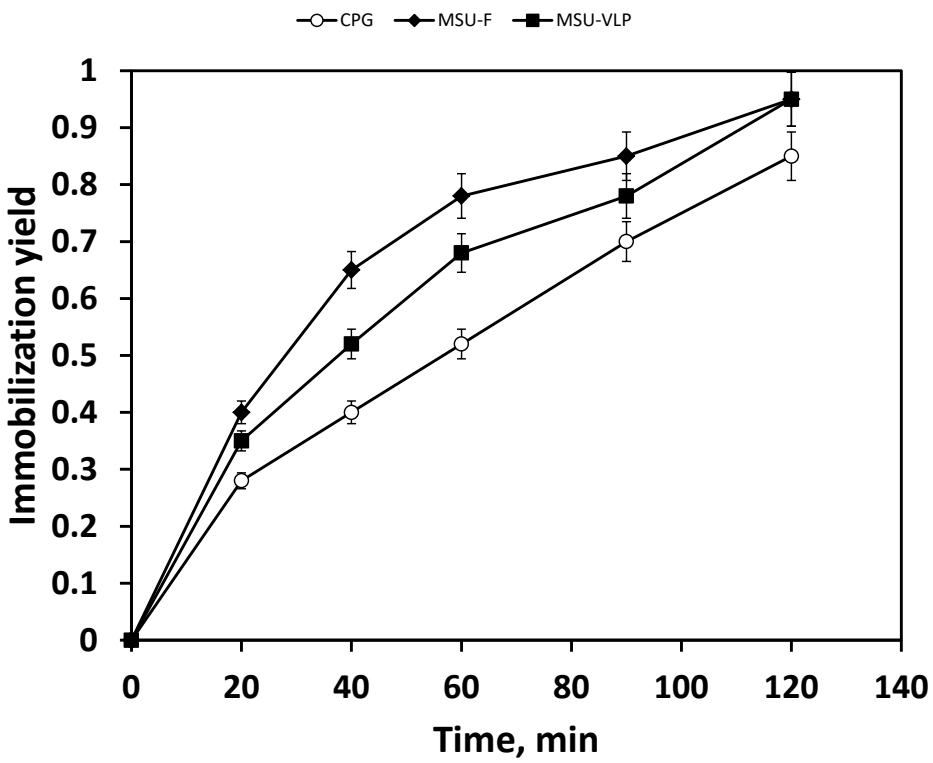

Figure S3. Course of immobilization of Zbasic2_DAAO on different silica supports. The enzyme loading was 1000 U/g_support. One unit (U) equals a rate of 1 μmol/min.

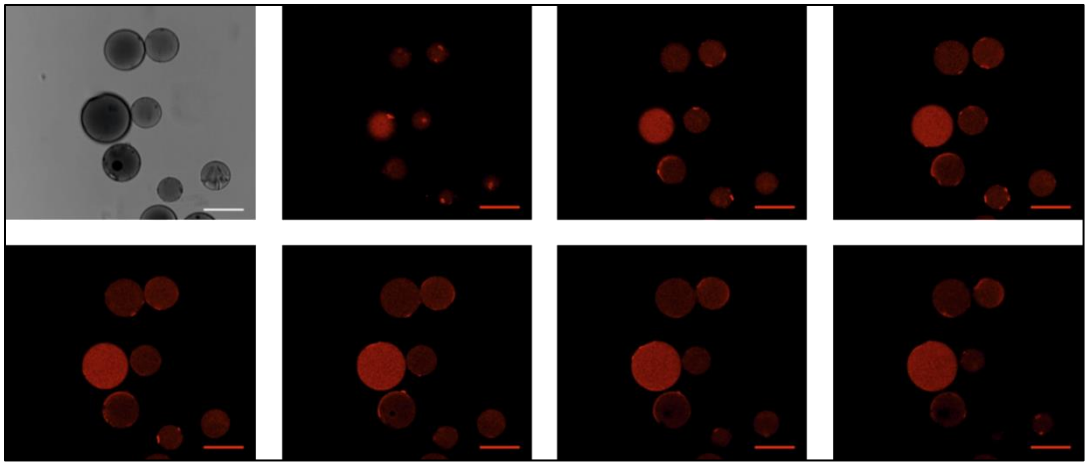

Figure S4. Confocal fluorescence images of CPG labeled heterogeneously with $Ru(dpp)_3$. The scale bar on the picture indicates a width of 100 µm. The first picture of each panel shows a transmission microscope image. The following pictures of each panel show fluorescence confocal images. The confocal fluorescence images were sustained by taking different deep z-section scans with 5 µm depth margin between each image.

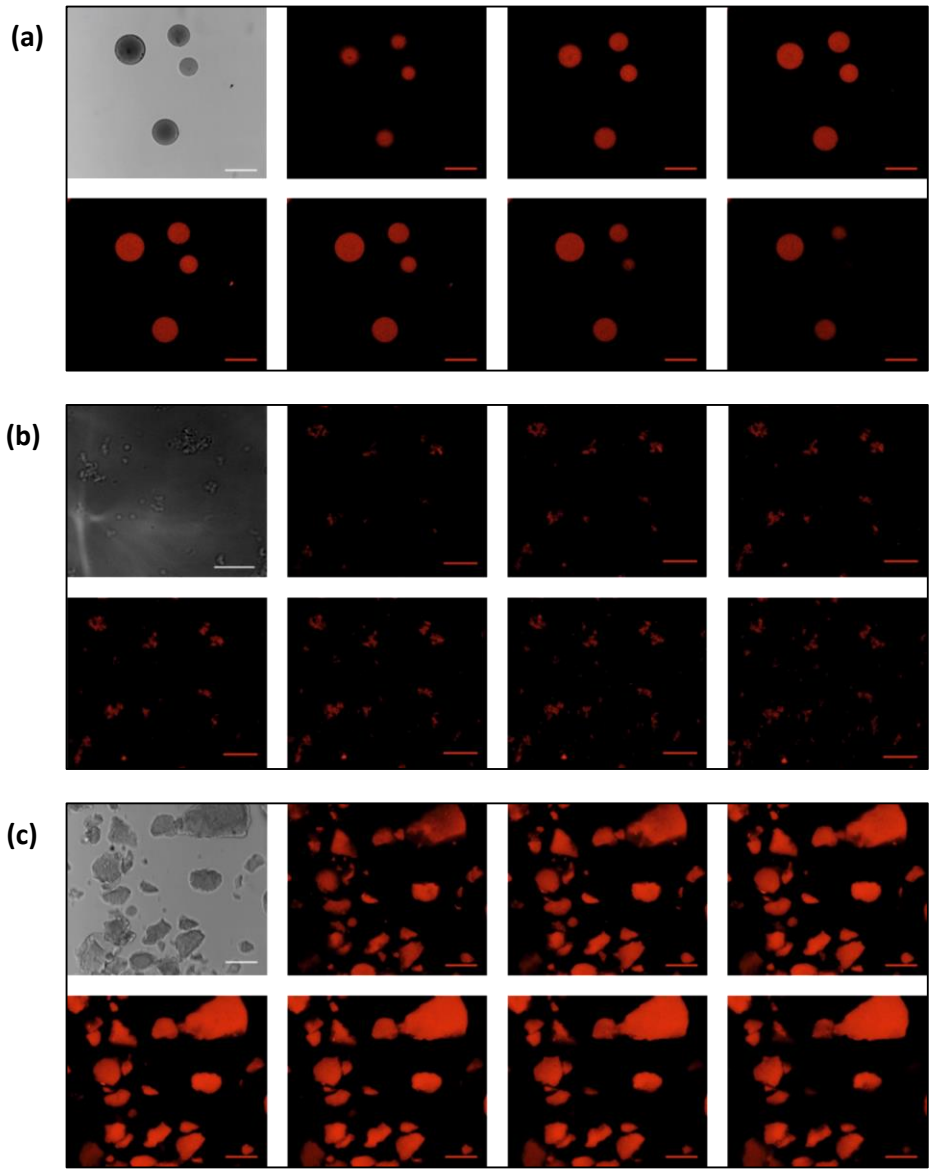

Figure S5. Confocal fluorescence images of silica materials labeled with $Ru(dpp)_3$. (a) CPG; (b) MSU-F; (c) MSU-VLP. The scale bar on the picture indicates a width of 100 μm for CPG and MSU-VLP and a width of 20 μm for MSU-F. The first picture of each panel shows a transmission microscope image. The following pictures of each panel show fluorescence confocal images. The confocal fluorescence images were sustained by taking different deep z-section scans with 0.33 (for MSU-F) or 4.99 μm (for CPG and MSU-VLP) depth margin between each image.

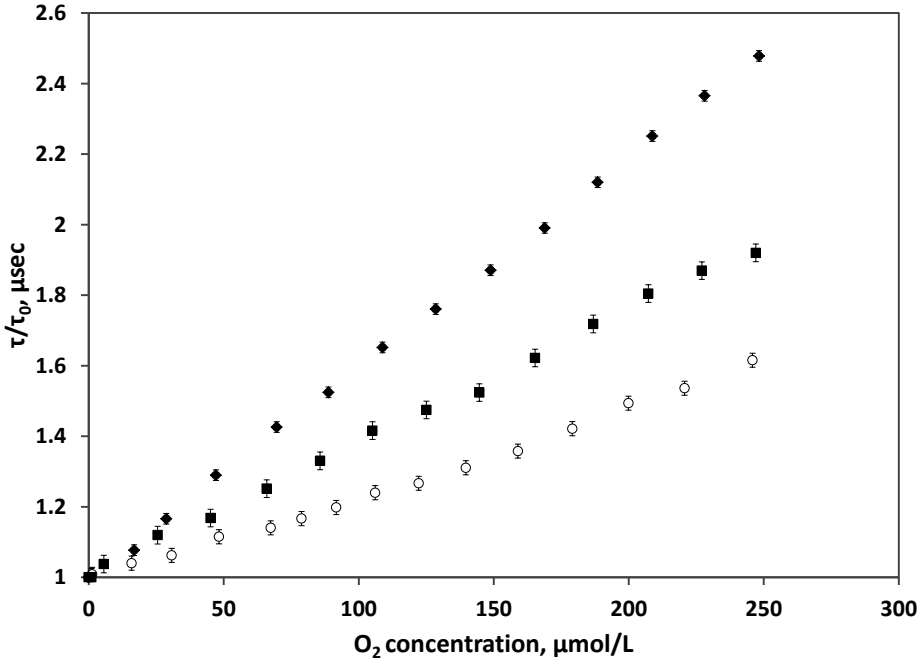

Figure S6. Correlation between luminescence lifetime of $Ru(dpp)_3$ adsorbed into silica supports and O_2 concentration in bulk liquid calibration. Figure shows the ratio of the lifetime under fully deoxygenated conditions and the measured lifetime. Circles refer to CPG derivatives; squares refer to MSU-VLP derivatives; diamonds refer to MSU-F derivatives. The correlation was obtained a DAAO catalyst contained 800 µmol/(min g_support) of maximum activity. Details about the set-up used to acquire luminescence lifetime data can be found in the Experimental Section of the main text.

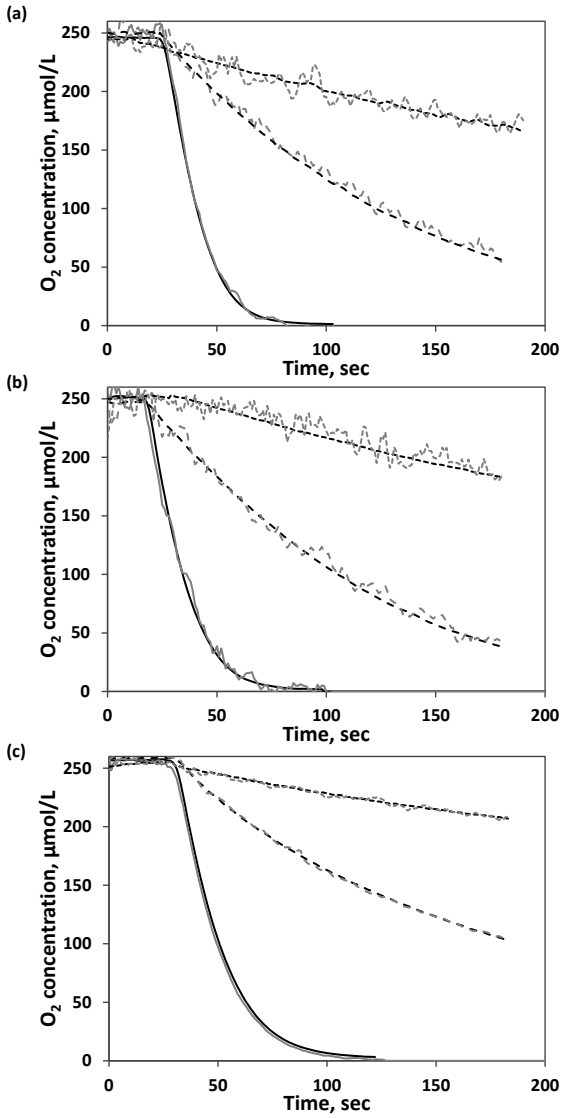

Figure S7. External (grey line) and internal (black line) course of the O_2 concentration, during oxidation of L-lactate catalyzed by soluble lactate oxidase. **(**a**)** CPG; (b) MSU-VLP; (c) MSU-F. Phosphorescent labeled silica materials containing immobilized Z_{basic2} _DAAO were used in a concentration of 5 mg/mL. A 50 mM potassium phosphate buffer, pH 8.0, was used, and the temperature was 30 °C. The supports were incubated in the presence with 50 mM L-lactate. The reaction was started by the addition of soluble lactate oxidase at different catalytic activities.

Continuous line shows results with 0.5 μmol/(min mL); dashed line shows results with 0.1 μmol/(min mL); square dotted line shows results with 0.025 μmol/(min mL).

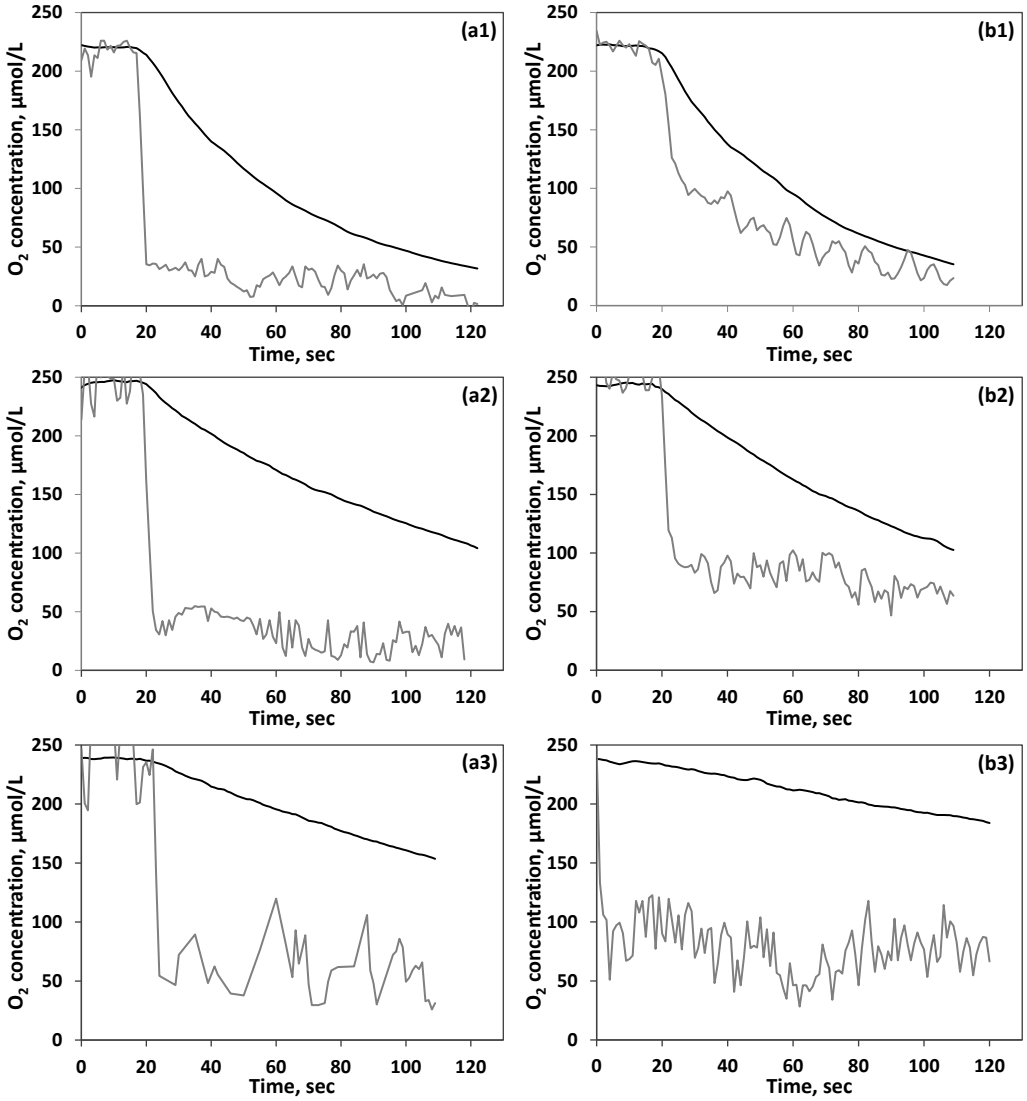

Figure S8. Time courses of the O_2 concentration in homogeneous liquid phase (black line) and intraparticle (grey line) monitored during oxidation of D-Met catalyzed by Zbasic2_DAAO immobilized into CPG. The catalyst loading was 5 mg_support/mL for row 1, 2.5 mg_support/mL for row 2 and 1.25 mg_support/mL for row 3. Columns a and b show results for a catalyst containing 800 µmol/(min g_support) and 300 µmol/(min g_support) of maximum activity respectively. Reactions were performed at 30 ºC and air saturated potassium phosphate 50 mM, pH 8.0. Time courses of internal O_2 concentration were biphasic where a fast drop was followed by gradual decrease in the O_2 concentration paired with O_2 concentration decrease in bulk phase. Graphs were used for the determination of dynamic O_2 gradient under pseudo steady state conditions after this first abrupt decrease. The quantification of O_2 under steady state was

performed using repeated time courses where maximum SD of 10 % was found. The data shown are an exemplary representation of multiple experiments carried out.

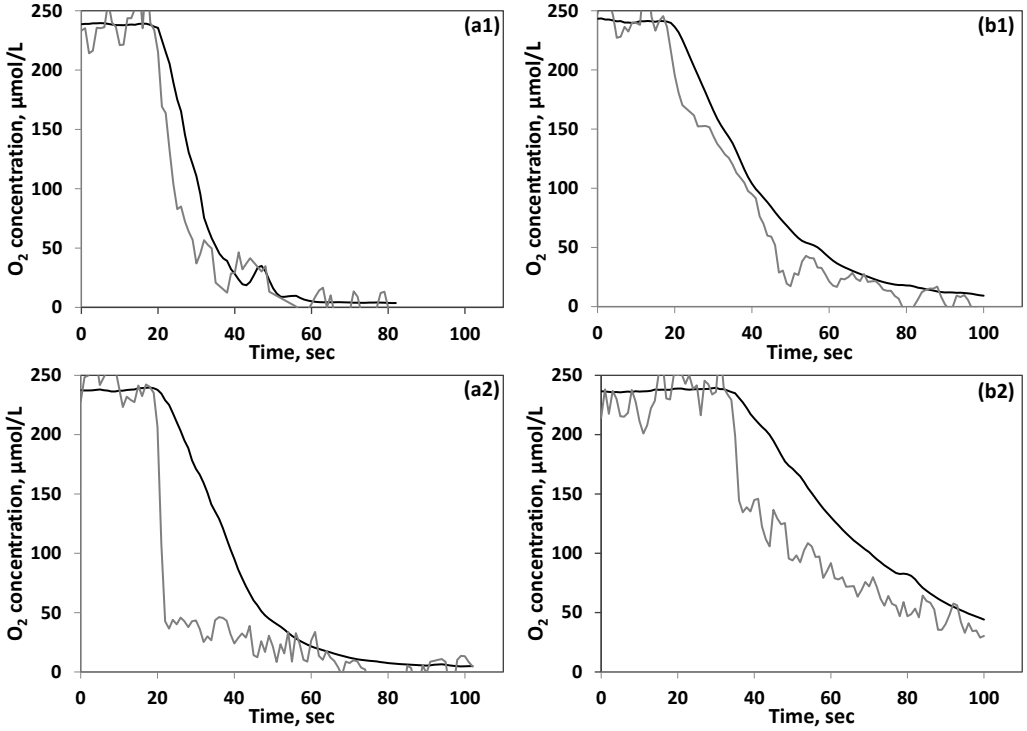

Figure S9. Time courses of the O_2 concentration in homogeneous liquid phase (black line) and intraparticle (grey line) monitored during oxidation of D-Met catalyzed by Zbasic2_DAAO immobilized into MSU-VLP. The catalyst loading was 5 mg_support/mL for row 1 and 2.5 mg_support/mL for row 2. Columns a and b show results for a catalyst containing 800 µmol/(min g_support) and 300 µmol/(min g_support) of maximum activity respectively. Reactions were performed at 30 ºC and air saturated potassium phosphate 50 mM, pH 8.0. Time courses of internal O_2 concentration were biphasic where a fast drop was followed by gradual decrease in the O_2 concentration paired with O_2 concentration decrease in bulk phase. Graphs were used for the determination of dynamic O_2 gradient under pseudo steady state conditions after this first abrupt decrease. The quantification of O_2 under steady state was performed using repeated time courses where maximum SD of 10 % was found. The data shown are an exemplary representation of multiple experiments carried out.

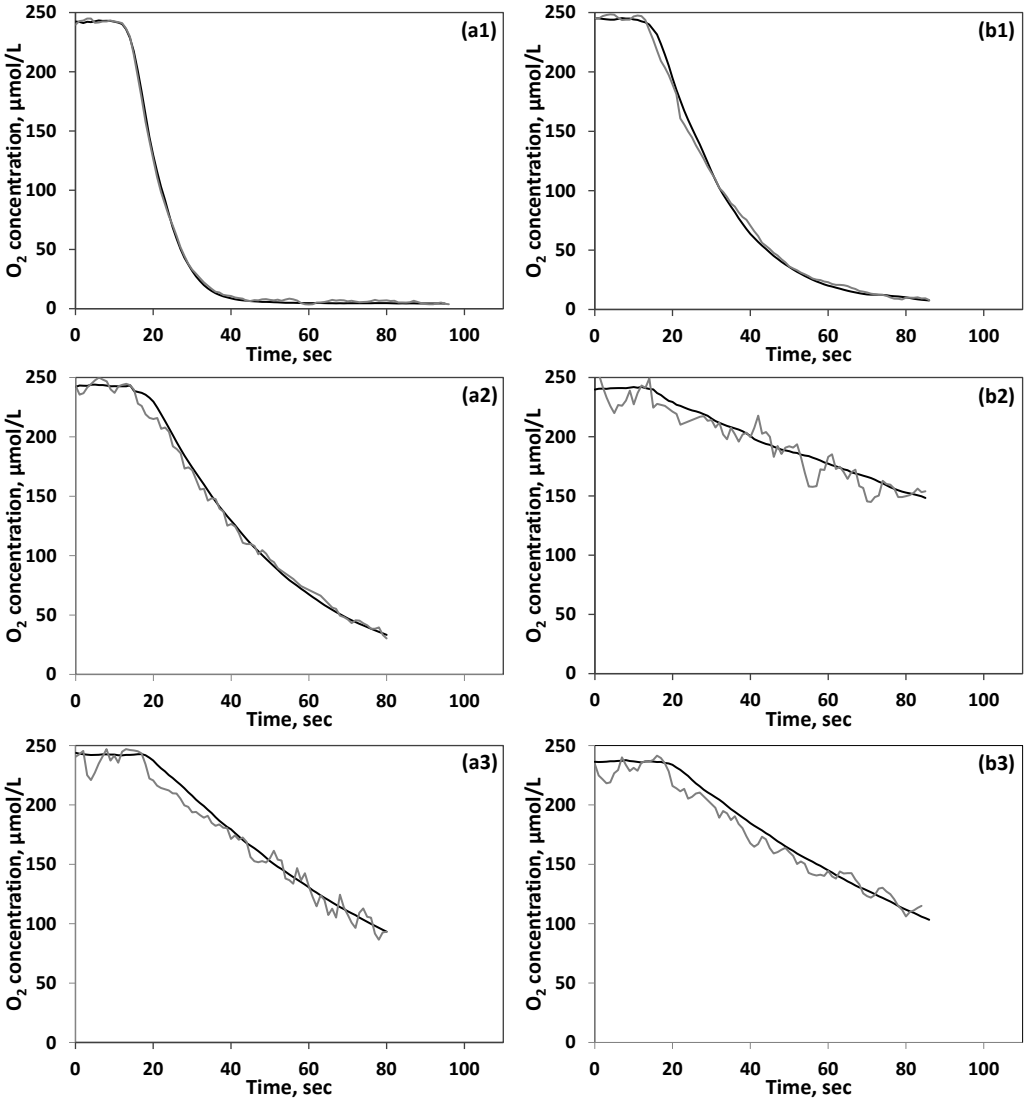

Figure S10. Time courses of the O_2 concentration in homogeneous liquid phase (black line) and intraparticle (grey line) monitored during oxidation of D-Met catalyzed by Zbasic2_DAAO immobilized into MSU-F. The catalyst loading was 5 mg_support/mL for row 1, 1.25 mg_support/mL for row 2 and 0.625 mg_support/mL for row 3. Column a and b show results for a catalyst containing 800 µmol/(min g_support) and 300 µmol/(min g_support) of maximum activity respectively. Reactions were performed at 30 ºC and air saturated potassium phosphate 50 mM, pH 8.0. Time courses of internal O_2 concentration were biphasic where a fast drop was followed by gradual decrease in the O_2 concentration paired with O_2 concentration decrease in bulk phase. Graphs were used for the determination of dynamic O_2 gradient under pseudo steady state conditions after this first abrupt decrease. The quantification of O_2 under steady state was

performed using repeated time courses where maximum SD of 10 % was found. The data shown are an exemplary representation of multiple experiments carried out.

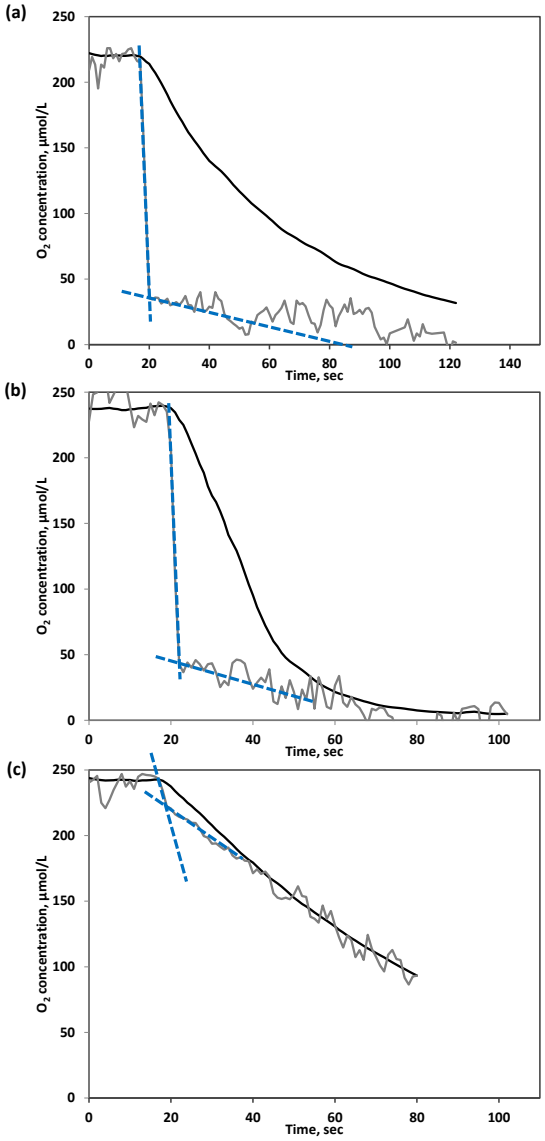

Figure S11. Determination of the maximum value of ΔO_2 in reactions catalyzed by different Time courses of the internal O_2 concentration were biphasic where a fast drop of the O_2 concentration was followed by a much slower decrease in the O_2 concentration. Tangents were constructed to the time courses of the fast phase and the immediately following slower phase. Intersection point of the two lines is used to obtain the maximum value of ΔO_2. The fast initial drop of the internal O_2 concentration which occurred at the limit of time resolution of the analytical method used was highly reproducible in magnitude (relative SD_10%) in repeated time-course experiments (N≥5). The data shown are representative of the multiple experiments carried out. Z_{basic2}_DAAO immobilizates containing 600 µmol/(min g_support) of maximum activity. (a) CPG; (b) MSU-

VLP; (c) MSU-F. The catalyst loading was 5 mg_support/mL. Reactions were performed at 30 ºC and aerated potassium phosphate (50 mM, pH 8.0) was used.

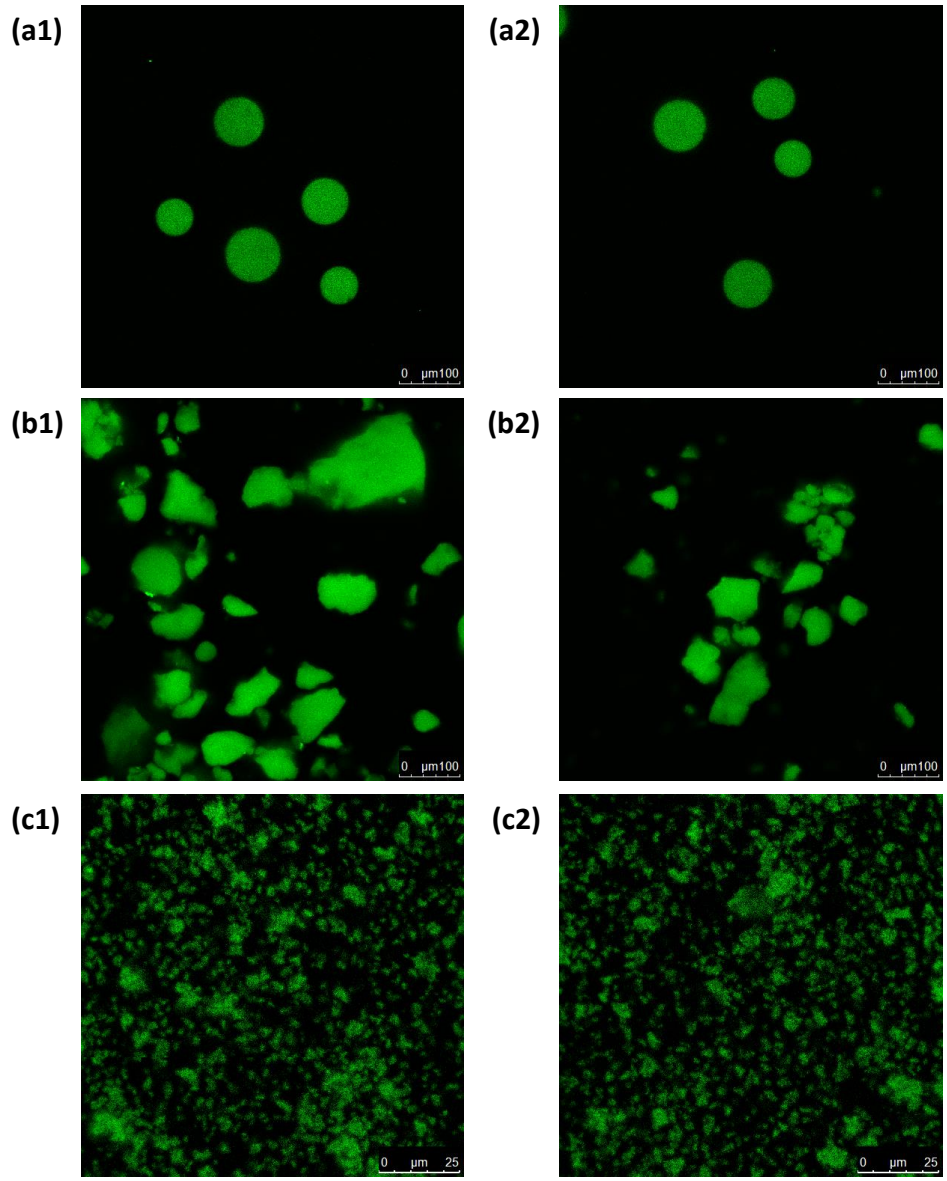

Figure S12. Confocal fluorescence images of silica materials labeled with Ru(dpp)3 before (Column 1) and after (Column 2) stirring experiments. (a) CPG; (b) MSU-VLP; (c) MSU-F. Luminophor labeled silica supports containing immobilized Zbasic2_DAAO were used for the determination of observable activity and determination of internal O2 concentration under stirring conditions as described in Experimental Section.